

are the minimum level of interaction needed for the optimal activity even if these interactions are not the sole determinant for the binding affinity.

In conclusion, the hydration free energies calculated using the hydration shell model on some 7-substituted 1-ethyl-6-fluoro-1,4-dihydro-4-oxoquinoline-3-carboxylic acids show some correlations with their inhibitory activities against DNA gyrase. The calculated dipole moments and charge distributions with CNDO/2 (ON) method do not show any correlations with the activities. The results may serve as a starting step for further studies in understanding the detailed binding affinity and specificity of quinolone analogues with DNA gyrase.

## References

1. P. B. Fernandes, *Quinolones*, J. R. Prous Science, Spain, 1989.
2. J. M. Domagala, L. D. Hanna, C. L. Heifetz, M. P. Hutt, T. F. Mich, J. P. Sanchez, and M. Solomon, *J. Med. Chem.*, **29**, 394 (1986).
3. G. Klopman, O. T. Macina, M. E. Levinson, and H. S. Rosenkranz, *Antimicrob. Agents Chemother.*, **31**, 1831 (1987).
4. L. L. Shen, L. A. Mitscher, P. N. Sharma, D. W. T. Chu, C. S. Cooper, T. Rosen, and A. G. Pernet, *Biochemistry*, **28**, 3886 (1989).
5. *Alchemy II*, Tripos Associates, Inc., 1988.
6. N. L. Allinger and Y. H. Yuh, *QCPE* **395**, 1980.
7. J. F. Yan, F. A. Momany, R. Hoffmann, and H. A. Scheraga, *J. Phys. Chem.*, **74**, 420 (1970).
8. Y. K. Kang, K. D. Gibson, G. Nemethy, and H. A. Scheraga, *J. Phys. Chem.*, **92**, 4739 (1988).
9. A. Bondi, *J. Phys. Chem.*, **68**, 441 (1964).

## Preparation, Structure, and Photoemission Studies on the High Temperature Superconductor $\text{YBa}_2\text{Cu}_{3-x}\text{Ni}_x\text{O}_{7-\delta}$

Jin-Ho Choy\* and Won-Young Choe

Department of Chemistry, Seoul National University, Seoul 151-742. Received April 9, 1990

$\text{YBa}_2\text{Cu}_{3-x}\text{Ni}_x\text{O}_{7-\delta}$  with  $x = 0.05, 0.2, 0.4, 0.7$  and  $1.0$  had been prepared by the thermal decomposition of corresponding nitrates. Among them, the sample with  $x = 0.05$  shows above-liquid- $\text{N}_2$  temperature superconductivity with  $T_c$  of 88.7K. According to the X-ray diffraction analysis, its crystal symmetry was estimated as orthorhombic with the lattice parameters of  $a = 3.866\text{\AA}$ ,  $b = 3.893\text{\AA}$ ,  $c = 11.715\text{\AA}$ . The chemical composition of the sample was determined by electron probe microanalysis and the chemical composition around its grain boundaries was carefully studied by the X-ray line scanning technique. From the observed binding energy of Ni- $2p_{3/2}$  orbital electron (B.E. = 853 eV) measured by X-ray photoelectron spectroscopy, the valency state of nickel stabilized in  $\text{YBa}_2\text{Cu}_{2.95}\text{Ni}_{0.05}\text{O}_{7-\delta}$  oxide lattice could be determined to be Ni(II).

## Introduction

$\text{YBa}_2\text{Cu}_3\text{O}_{7-\delta}$  ( $0 < \delta < 0.5$ ) is superconducting<sup>1</sup> above 90 K and has a threefold stacked perovskite structure where the central perovskite unit contains Y while two remaining units contain Ba. Neutron and X-ray diffraction studies<sup>2-5</sup> on the various oxygen contents clearly show that  $\text{YBa}_2\text{Cu}_3\text{O}_{7-\delta}$  undergoes an orthorhombic-to-tetragonal phase transition<sup>6,7</sup> at around  $\delta = 0.5$  with the drastic diminution of  $T_c$  as oxygen disintercalates out of the Cu(1) plane between Ba layers. It becomes now evident that in the  $\text{YBa}_2\text{Cu}_3\text{O}_{7-\delta}$  oxide its physical and structural properties depend strongly on its oxygen content and on two dimensional sheets of Cu-O pyramids or one dimensional chains. Additionally, the influence of other cations in  $\text{YBa}_2\text{Cu}_3\text{O}_{7-\delta}$  has been investigated by the perturbation of the perovskite structure through isomorphous substitutions<sup>3, 8-12</sup>. The substitution of magnetic rare earth cations for Y clearly shows that the Y site in the lattice has only a minor effect on  $T_c$ <sup>3</sup>, which suggests the superconductivity develops far from the Y site. However, tremendous decrease in  $T_c$  was observed from the substitution of 3d transition metal for Cu<sup>8-12</sup>. Band structure cal-

culations<sup>13</sup> performed on this Y-Ba-Cu-O system also led to the conclusion that the  $\text{Cu}3d-(\text{O}2p)$  electrons govern the superconducting properties of this oxide. To understand the mechanism of the superconductivity further on Y-Ba-Cu-O system, it is necessary to study the cation substitution effect for Cu sites along with careful physical characterization. Among the cations substituted, Ni ion is known to occupy preferentially the Cu(2) site in the Y and Ba layers<sup>14</sup> and give only a moderate decrease of  $T_c$ <sup>15</sup> as shown in Figure 1. Regardless of enormous researches on the Ni substitution for Cu, only a few papers<sup>16,17</sup> have discussed on their physical characterizations.

In this paper, we present X-ray diffraction, electron probe microanalysis and X-ray photoelectron spectroscopic studies on  $\text{YBa}_2\text{Cu}_{2.95}\text{Ni}_{0.05}\text{O}_{7-\delta}$  to estimate the actual site of Ni in the lattice and to gain the information on the role of two different sites of Cu in the lattice through the substitution of Ni ion.

## Experimental

Samples of  $\text{YBa}_2\text{Cu}_{3-x}\text{Ni}_x\text{O}_{7-\delta}$  with  $x = 0.05, 0.2, 0.4, 0.7$ ,

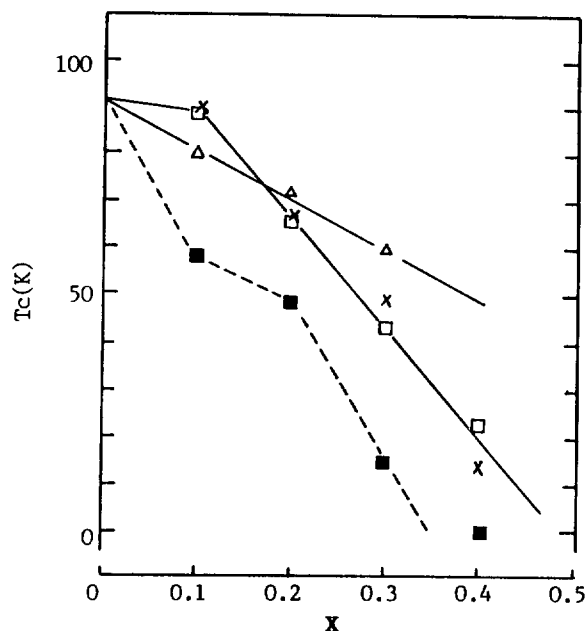


Figure 1.  $T_c$  vs  $x$  relations for  $\text{YBa}_2\text{Cu}_{3-x}\text{M}_x\text{O}_{7-\delta}$ .

and 1.0 were prepared by decomposition of the corresponding nitrates. Stoichiometric mixtures of  $\text{Y}_2\text{O}_3$ ,  $\text{Ba}(\text{NO}_3)_2$ , Cu powder and  $\text{Ni}(\text{NO}_3)_2$  were dissolved in an aqueous solution of nitric acid and the resulting samples were evaporated to dryness at  $150^\circ\text{C}$  and heated at  $700^\circ\text{C}$  for 1 hour to decompose the nitrates. It were then well-ground, pelletized, calcined at  $900^\circ\text{C}$  for 16 hours, sintered at  $950^\circ\text{C}$  for 16 hours with two intermediate grindings, and finally annealed at  $450^\circ\text{C}$  for 16 hours in oxygen atmosphere.

The structural analysis of the prepared samples was performed by Jeol X-ray powder diffractometer with Ni-filtered  $\text{Cu-K}\alpha$  radiation ( $\lambda = 1.5418 \text{ \AA}$ ). Lattice parameters were determined by standard least square method from  $2\theta$  values and corrected by the internal standard of NaCl.

Chemical composition and microstructure of the sample was analyzed with a scanning electron microscope (SEM), Jeol-JSM-840 A, equipped with an energy dispersive spectrometer (EDS), which allows a quantitative analysis of different phases present in the sample.

X-ray photoelectron (XPE) spectroscopy measurements were performed with a PHI 5100 Perkin-Elmer spectrometer which has been calibrated by  $\text{Ag}3d_{5/2}$ ,  $\text{Ag}3d_{3/2}$ ,  $\text{Au}4f_{7/2}$  and carbon 1s core level energy. The binding energies reported here were corrected from the known reference (B.E. of  $\text{C}1s = 284.6 \text{ eV}$ ). Unmonochromatized  $\text{Mg-K}\alpha$  radiation of  $1253.6 \text{ eV}$  was used and the base pressure of sample chamber in the spectrometer was lower than  $2.0 \times 10^{-9}$  torr.

## Results and Discussion

Figure 2 shows the X-ray diffraction patterns for  $\text{YBa}_2\text{Cu}_{3-x}\text{Ni}_x\text{O}_{7-\delta}$ . The X-ray diffraction patterns for  $x \leq 0.4$  show that the sintered samples are single phase without detectable impurities such as  $\text{BaCuO}_2$  and  $\text{Y}_2\text{Cu}_2\text{O}_5$ , but those for  $x \geq 0.7$  are similar to the amorphous phase without forming any superconducting  $\text{YBa}_2\text{Cu}_3\text{O}_{7-\delta}$  phase. According to the previous report<sup>18</sup> on the solubility limit of Ni for Cu in  $\text{YBa}_2\text{Cu}_3\text{O}_{7-\delta}$  matrix, maximum concentration of Ni soluble

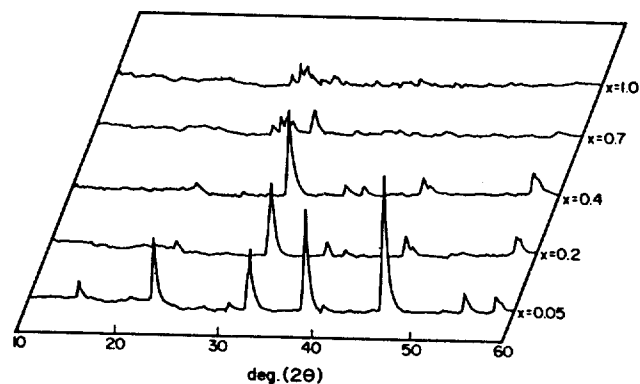


Figure 2. X-ray diffraction patterns for  $\text{YBa}_2\text{Cu}_{3-x}\text{Ni}_x\text{O}_{7-\delta}$  where  $x = 0.05, 0.2, 0.4, 0.7, 1.0$ .

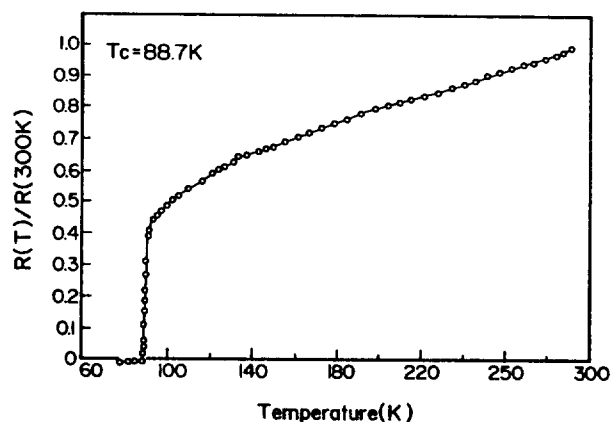
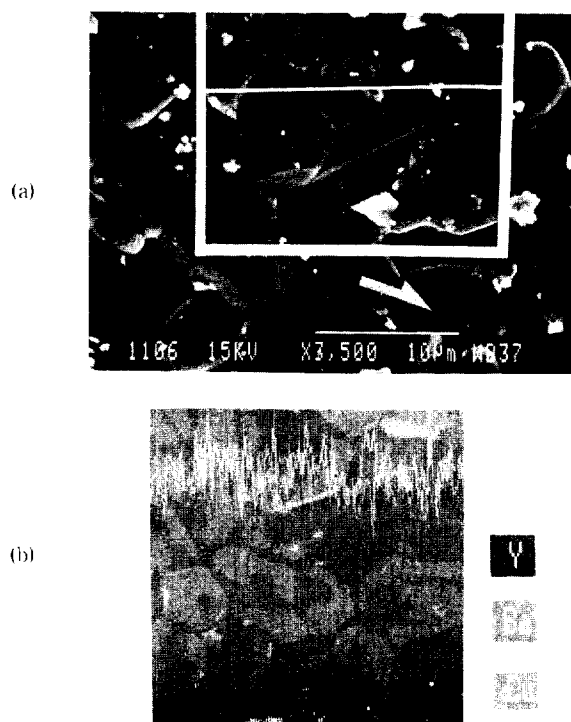


Figure 3. Normalized resistance vs. temperature from 300 K to 77 K for  $\text{YBa}_2\text{Cu}_{2.95}\text{Ni}_{0.05}\text{O}_{7-\delta}$ .

to the lattice is expected to be about  $x = 0.3$ , which is somewhat smaller value than the present results ( $x \approx 0.4$ ). Compared with the X-ray diffraction patterns of the Ni-rich samples,  $\text{YBa}_2\text{Cu}_{2.95}\text{Ni}_{0.05}\text{O}_{7-\delta}$  exhibits strong enhancement of  $(00l)$  reflections, where  $l$  is an integer. This phenomenon can be explained by strong tendency to  $c$ -axis orientation to the pressed surface of the pellet. This  $c$ -axis orientation is often observed in the sample prepared by not only special technique like chemical vapor deposition<sup>19</sup>, but also common method like solid state reaction<sup>20</sup>. In case where the  $c$ -axis orientation appears, it was reported that the critical current density is strongly enhanced by one and half times compared with unoriented sample<sup>21</sup>. According to the electrical resistance measurements, only the sample with the nominal composition  $\text{YBa}_2\text{Cu}_{2.95}\text{Ni}_{0.05}\text{O}_{7-\delta}$  shows superconductivity above liquid  $\text{N}_2$  temperature (Figure 3) and this result is in good agreement with the relation associated with  $T_c$  and Ni concentration in Figure 1. The superconducting off-set temperature for  $x = 0.05$  is  $88.7 \text{ K}$  and it is slightly lower value than the undoped sample as expected.

The sample with nominal composition  $\text{YBa}_2\text{Cu}_{2.95}\text{Ni}_{0.05}\text{O}_{7-\delta}$  was analyzed to know its true chemical composition and microstructure using a SEM equipped with EDS<sup>22</sup>. Figure 4(a) represents a SEM image of the sample  $\text{YBa}_2\text{Cu}_{2.95}\text{Ni}_{0.05}\text{O}_{7-\delta}$ . Table 1 shows relative atom concentrations with respect to Y, Ba and Cu on the spot indicated by the arrow in Figure 4(a). The chemical composition of the spot is identical to un-



**Figure 4.** Scanning electron micrograph (a) and X-ray line scanning (b) of  $\text{YBa}_2\text{Cu}_{2.95}\text{Ni}_{0.05}\text{O}_{7-\delta}$ .

**Table 1.** EDS Analysis with Respect to Y, Ba and Cu on the Spot Indicated by an Arrow in Figure 3(a)

	Y	Ba	Cu	O
atom percent (%)	7.61	16.72	23.77	51.90
mole ratio	1.0	2.1	3.1	6.7
ideal mole ratio	1.00	2.00	2.95	—

**Table 2.**  $\text{Ni-}2p_{3/2}$  Binding Energies for Ni-Compounds

Compound	$\text{Ni-}2p_{3/2}$ (eV)	Ref.
Ni metal	852.5	24
NiO	854.0	25
$\text{YBa}_2\text{Cu}_{2.95}\text{Ni}_{0.05}\text{O}_{7-\delta}$	853.3	this work
$\text{Ni}_2\text{O}_3$	855.6	26

doped  $\text{YBa}_2\text{Cu}_3\text{O}_{7-\delta}$  approximately and Ni dopant could not be detected due to its low concentration (about 0.1 atom percent) which is far below the detection limit of EDS. In order to test the homogeneity of the sample, X-ray line scanning analysis was also performed. X-ray line scanning in the Figure 4(b) represents relative atomic concentration qualitatively by peaks up (high concentration) and down (low concentration) along the horizontal line in the Figure 4(a). As shown in the Figure 4(b), Ba and Cu concentrations are nearly constant along the line. However, Y concentration changes remarkably in the grain boundaries due to the existence of Cu-rich phases such as  $\text{BaCuO}_2$  and  $\text{CuO}$ . The Cu-rich impurity phases in the grain boundaries are unavoidable due to their low melting temperature.<sup>23</sup>

XPE spectroscopy was performed to estimate the valency

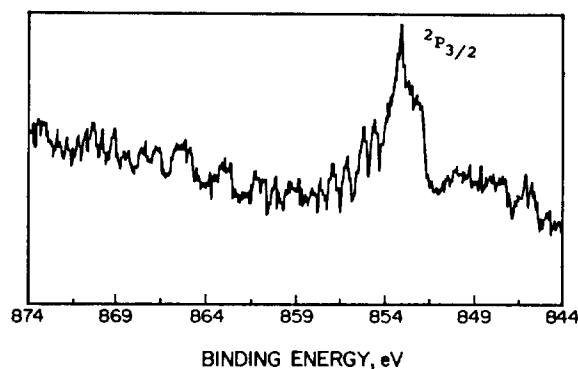


**Figure 5.** XPE spectrum in the region of the binding energy for Ni  $2p$  electrons in  $\text{YBa}_2\text{Cu}_{2.95}\text{Ni}_{0.05}\text{O}_{7-\delta}$ .

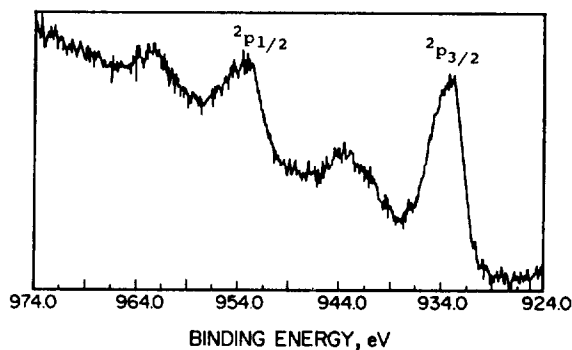


**Figure 6.** XPE spectrum in the region of the binding energy for Cu  $2p$  electrons in  $\text{YBa}_2\text{Cu}_{2.95}\text{Ni}_{0.05}\text{O}_{7-\delta}$ .

state of Ni stabilized in the  $\text{YBa}_2\text{Cu}_{2.95}\text{Ni}_{0.05}\text{O}_{7-\delta}$  lattice. Because of the low atomic concentration of Ni in  $\text{YBa}_2\text{Cu}_3\text{O}_{7-\delta}$  matrix, the accumulation time for Ni should be required three times as much as that for other elements. Figure 5 show the XPE spectra for Ni in the binding energy range of  $2p_{3/2}$  electrons. Small but significant peak is observed at 853.3 eV, which is lower than  $2p_{3/2}$  peak of NiO by 0.7 eV. Compared with  $2p_{3/2}$  binding energy for divalent and trivalent nickel in the oxide lattice (Table 2),  $\text{Ni}_2\text{O}_3$  has higher  $2p_{3/2}$  binding energy than NiO by 1.6 eV. Hence the observed binding energy of the Ni- $2p_{3/2}$  electrons in  $\text{YBa}_2\text{Cu}_{2.95}\text{Ni}_{0.05}\text{O}_{7-\delta}$  is quite close to those of divalent nickel compounds. A slight shift of Ni binding energy to a low energy site could be ascribed to an electron delocalization from the fact that it has an intrinsic metal-like property ( $R \approx 10^{-3} \Omega$ ). Therefore the valency state of Ni in  $\text{YBa}_2\text{Cu}_{2.95}\text{Ni}_{0.05}\text{O}_{7-\delta}$  could be assigned to be divalent. This result is consistent with the experimental fact that oxygen content does not change upon substitution for Cu by Ni using thermogravimetric analysis.<sup>27</sup>

The XPE spectrum of Cu  $2p$  region at room temperature is presented in Figure 6. The Cu  $2p$  core level spectrum for the sample shows two main peaks corresponding to  $2p_{1/2}$  and  $2p_{3/2}$  levels, accompanied by satellite peaks at higher binding energy of about 9 eV than the main  $2p$  peaks. Such satellites are frequently observed in core-level photoemission from divalent copper compounds<sup>28-30</sup> and are attributed<sup>31</sup> to a ligand-to-metal charge transfer ( $2p^6 3d^9 \rightarrow 2p^5 3d^{10}$ ) in the final state of photoemission process, thereby effectively screening the excited core hole. The existence of these

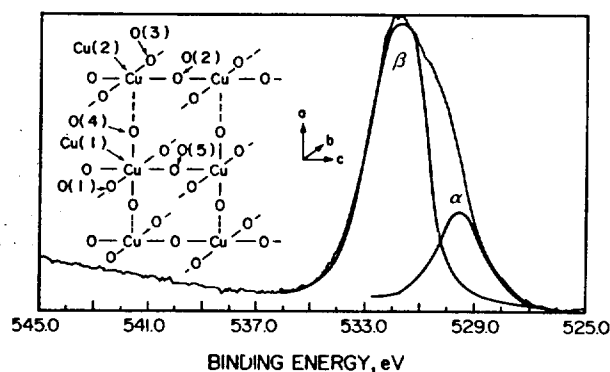


**Figure 7.** Peak separation in the region of the binding energy for O1s electrons in  $\text{YBa}_2\text{Cu}_{2.95}\text{Ni}_{0.05}\text{O}_{7-\delta}$ .

satellites strongly supports the presence of  $\text{Cu}^{2+}$  or higher oxidation state of Cu. Although we could not find direct evidence for  $\text{Cu}^{3+}$  ions from the spectra, the broad line shape of the  $2p_{3/2}$  peak is partly ascribed to two distinct oxidation state of Cu ( $\text{Cu}^{2+}$  and  $\text{Cu}^{3+}$ ) in the unit cell<sup>32,33</sup>.

The O1s spectrum for  $\text{YBa}_2\text{Cu}_{2.95}\text{Ni}_{0.05}\text{O}_{7-\delta}$  consisted of two main contributions are 529.6 eV and 532.1 eV as indicated by  $\alpha$  and  $\beta$  in Figure 7, respectively.

In the crystal structure of  $\text{YBa}_2\text{Cu}_3\text{O}_{7-\delta}$ , there exists three different coordination environments of oxygen in the unit cell: O(1) (or O(5)) between two Cu(1) sites, O(2) (or O(3)) between two Cu(2) sites, and O(4) between Cu(1) and Cu(2) site. In spite of different chemical environment of oxygen, the spectra of O1s region are overlapped one another and consequently represent a broad singlet O1s peak in the undoped  $\text{YBa}_2\text{Cu}_3\text{O}_{7-\delta}$  sample<sup>34</sup>. As the crystal structure undergoes a distortion (due to the orthorhombic-to-tetragonal phase transition or isomorphous substitution in the lattice), O1s peak in the XPE spectrum begins to separate. If Ni(II) ions occupy the Cu(2) sites, two oxygen sites directly connected with Cu(2) one (i.e., O(2) (or O(3)) and O(4)) should be influenced greatly. From these considerations, an additional peak at around 530 eV could be assigned as the peak corresponding to the oxygen in the Cu(2) plane.

**Acknowledgement.** This research is supported by the Korean Ministry of Science and Technology (MOST).

## References

1. M. K. Wu, J. R. Ashburn, C. J. Torng, P. H. Hor, R. L. Meng, L. Gao, Z. J. Huang, Y. Q. Wang, and C. W. Chu, *Phys. Rev. Lett.*, **58**, 908 (1987).
2. J. D. Jorgensen, M. A. Beno, D. G. Hinks, L. Soderholm, K. J. Volin, R. L. Hitterman, D. G. Grace, I. K. Schuller, C. U. Serge, K. Zhang, and M. S. Kleefisch, *Phys. Rev.*, **B36**, 3608 (1987).
3. J. D. Jorgensen, B. W. Veal, W. K. Kwok, G. W. Crabtree, A. Umezawa, L. J. Nowicki, and A. P. Paulikas, *Phys. Rev.*, **36**, 5731 (1987).
4. J. M. Tarascon, W. R. Mckinnon, L. H. Greene, G. W. Hull, and E. M. Vogel, *Phys. Rev.*, **B36**, 226 (1987).
5. I. K. Schuller, D. G. Hinks, M. A. Beno, D. W. Capone, H. L. Soderholm, J.-P. Locquet, Y. Bruynseraede, C. U. Segre, and K. Zhang, *Solid State Commun.*, **63**, 385 (1987).
6. J. M. Tarascon, P. Barboux, B. G. Bagley, L. H. Green, W. R. Mckinnon, and G. W. Hull, *Chemistry of high temperature superconductors*, American Chemical Society, Washington, DC, 1987, p. 198.
7. R. J. Cava, B. Batlogg, C. H. Chen, E. A. Rietman, S. M. Zahurok, and D. Werder, *Phys. Rev.*, **B36**, 5719 (1987).
8. J. M. Tarascon, W. R. Mckinnon, L. H. Greene, G. W. Hull, and E. M. Vogel, *Phys. Rev.*, **B36**, 16 (1987).
9. J. M. Tarascon, L. H. Green, B. G. Batlogg, W. R. Mckinnon, P. Barboux, and G. W. Hull, *Novel Superconductivity* Plenum, New York, 1987, p. 705.
10. G. Xiao, F. H. Streitz, A. Garrin, Y. W. Du, and C. L. Chien, *Phys. Rev.*, **B35**, 8782 (1987).
11. Y. Maeno, T. Tomita, M. Kyogoku, S. Awaji, Y. A. Ok, K. Hoshino, A. A. Minami, and T. Fujita, *Nature*, **328**, 512 (1987).
12. B. W. Veal, W. K. Kwok, A. Umezawa, G. W. Crabtree, J. D. Jorgensen, J. W. Downey, L. J. Nowicki, A. W. Mitchell, A. P. Paulikas, and C. H. Sowers, *Appl. Phys. Lett.*, **51**, 279 (1987).
13. L. F. Mattheis and D. R. Hamann, *Solid State Commun.*, **63**, 395 (1987).
14. T. Kajitani, K. Kusaba, M. Kikuchi, Y. Syono, and M. Hirabayashi, *Jpn. J. Appl. Phys.*, **26**, L1727 (1987).
15. E. Takayama-Muromachi, Y. Uchida, and K. Kato, *Jpn. J. Appl. Phys.*, **26**, L2087 (1987).
16. Y. Zhao, H. Zhang, and Zhang Qirui, *Physica C*, **162-164**, 47 (1989).
17. M. Kakihana, L. Borjesson, and S. G. Eriksson, *Physica C*, **162-164**, 1251 (1989).
18. Y. Maeno, T. Nojima, Y. Aoki, M. Kato, K. Hoshino, A. Minami, and T. Fujita, *Jpn. J. Appl. Phys.*, **26**, L774 (1987).
19. H. Yamane, H. Kurosawa, H. Iwasaki, H. Masumoto, T. Hirai, N. Kobayashi, and Y. Muto, *Jpn. J. Appl. Phys.*, **27**, L1275 (1988).
20. J.-H. Choy, W.-Y. Choe, and Q. W. Choi, *Mat. Res. Bull.*, **24**, 867 (1989).
21. Y. Enomoto, T. Murakami, M. Suzuki, and K. Moriwaki, *Jpn. J. Appl. Phys.*, **26**, L1248 (1987).
22. B. Yazar, J. Trefny, F. Schowenaardt, N. Mitra, and G. Pine, *Adv. Cer. Mat.*, **2**, 372 (1987).
23. R. W. McCallum, J. D. Verhoeven, M. A. Noack, E. D. Gibson, F. C. Laabs, and D. K. Finnemore, *Adv. Cer. Mat.*, **2(3B)**, 388 (1987).
24. L. J. Matino, L. I. Yu, S. O. Grim, and W. E. Swartz, Jr., *Inorg. Chem.*, **12**, 2762 (1973).
25. N. S. McIntyre and W. G. Cook, *Anal. Chem.*, **47**, 2208 (1975).
26. K. S. Kim, W. E. Baulinger, J. W. Amy, and N. Winograd, *Electron Spectrosc.*, **5**, 351 (1974).
27. Y. Shimakawa, Y. Kubo, K. Utsumi, Y. Takeda, and M. Takano, *Jpn. J. Appl. Phys.*, **27**, L1071 (1988).
28. C. D. Wagner, *Practical surface analysis by auger and x-ray photoelectron spectroscopy*, Wiley, Chichester, 1983.
29. T. Novakov, *Phys. Rev.*, **B3**, 269 (1971).
30. D. C. Frost, A. Ishitani, and C. A. McDowell, *Mol. Phys.*, **24**, 861 (1972).
31. A. Rosencwaig and G. K. Wertheim, *J. Electron Spectrosc.*, **1**, 493 (1972/73).

32. K. S. Kim, *J. Electron Spectrosc.*, **6**, 71 (1974).  
 33. H. Watanabe, K. Ikeda, H. Miki, and Ishida, *Jpn. J. Appl. Phys.*, **27**, 783 (1988).  
 34. H. Ihara, M. Jo, N. Terada, M. Hirabayashi, H.

Oyanagi, K. Murata, Y. Kimura, R. Sugise, I. Haya-shida, S. Oshashi, and M. Akimoto, *Physica C*, **153-154**, 131 (1988).

## New Thiazolo[3,2-*b*][1,2,4]triazole Derivatives: Useful Compounds for the Preparation of 7-Substituted Cephalosporins

Ghilsoo Nam, Jae Chul Lee, Dae Yoon Chi\*, and Joong-Hyup Kim\*

Korea Institute of Science and Technology, Seoul 130-650. Received April 9, 1990

We have synthesized several bicyclic heteroaromatic compounds with bridgehead nitrogen from N-amine salts of heteroaromatic amines. 2-Amino and 2-unsubstituted thiazolo[3,2-*b*][1,2,4]triazole derivatives **2a-b** were prepared by the cyclization reaction from N-amine salts of aminothiazole-5-yl(N-methoxyimino)acetate with cyanogen bromide and formamidine acetic acid salt, respectively. 2-Methylthiazolo[3,2-*b*][1,2,4]triazole **2c** was obtained from N-acetylated N-amine salt of aminothiazole-5-yl(N-methoxyimino)acetate by the cyclization reaction in the presence of polyphosphoric acid (PPA). 2-Substituted and 2-unsubstituted thiazolo[3,2-*b*][1,2,4]triazole derivatives **2a-c** were coupled with 7-aminocephalosporanic acid (7-ACA). Coupled cephalosporin derivatives **1a-c** did not have good antibacterial activities *in vitro*.

### Introduction

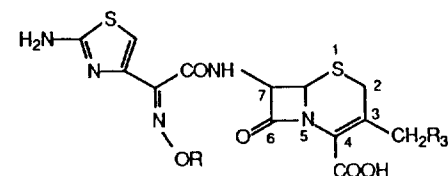
With the discovery of aminothiazole in the 7-side chain of cephalosporin by French workers (Bucourt *et al.*)<sup>1</sup> in 1977, it has been great interest to synthesize new cephalosporins which have better antibacterial activity than those having aminothiazole moiety in the 7-side chain. It has been known that any substituent of amino group of thiazole ring dramatically drops the antibacterial activity. In this report we have described the synthesis of several bicyclic heteroaromatic compounds with bridgehead nitrogen by the cyclization reaction from N-amine salts of aminothiazole-5-yl(N-methoxyimino)acetate with cyanogenbromide, formamidine acetic acid salt, and from N-acetylated N-amine salts of aminothiazole-5-yl(N-methoxyimino)acetate. 2-Substituted and 2-unsubstituted thiazolo[3,2-*b*][1,2,4]triazole derivatives **2a-c** were coupled with 7-aminocephalosporanic acid (7-ACA).

### Results and Discussion

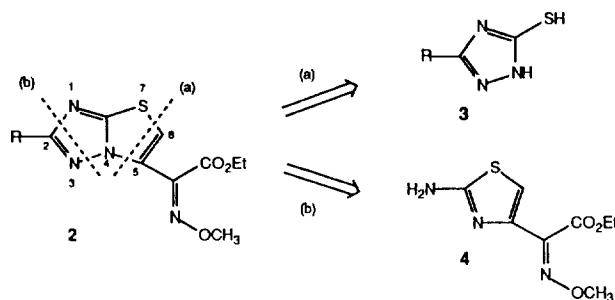
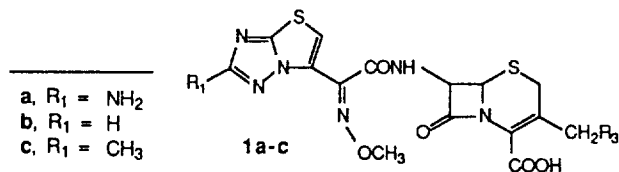
As illustrated in Scheme 1, ethyl (Z)-2-(2-substituted-thiazolo[3,2-*b*][1,2,4]triazol-5-yl)-2-(methoxy-imino)acetate analogues **2** can be synthesized by two different ring formations. By the first (route (a)), 3-mercaptotriazole is alkylated with ethyl 4-chloro-2-methoxyimino-3-oxobutynoate, followed by cyclodehydration. The alternative route (b), thiazolo[3,2-*b*][1,2,4]triazole ring can be prepared from aminothiazole derivative **4** by N-amination and cyclization of di-amino group. Basic ring systems of thiazolo[3,2-*b*][1,2,4]triazole with simple substituents has been synthesized by several workers and their synthetic methods were one of these two routes.<sup>2,3</sup>

#### 2-Aminothiazolo[3,2-*b*][1,2,4]triazole Derivative.

We have great interest for these amino derivatives, since 2-amino functional group in thiazole plays the important role for showing antibacterial activities. With route (a), 3-mercaptotriazole **3a** was reacted with chloroacetone as a model compound of 4-chloro-2-methoxyimino-3-oxobutynoate, providing 2-amino-5-methylthiazolo[3,2-*b*][1,2,4]triazole **6** via alkylated-uncyclized intermediate **5** as shown in Scheme



Aminothiazole Cephalosporin



Scheme 1